Primljen / Received: 26.12.2023.
Ispravljen / Corrected: 18.10.2024.
Prihvaćen / Accepted: 28.10.2024.
Dostupno online / Available online: 10.3.2025.

# Pre-fabricated design of transportable blast resistant composite concrete panels

Author:

Assoc.Prof. **Niyazi Özgür Bezgin**, PhD. CE
Istanbul University - Cerrahpaşa, Avcılar Campus
Department of Civil Engineering
Istanbul, Turkiye
ozgur.bezgin@iuc.edu.tr
**Corresponding author**

Research Paper

Niyazi Özgür Bezgin

## Pre-fabricated design of transportable blast resistant composite concrete panels

This study presents a design approach for 50 mm thick prefabricated composite concrete panels capable of withstanding blast pressures from C4-type explosives applied to their surfaces. The composite panel consists of a high-strength concrete core that is shear-bonded and positioned between two steel plates. The designed panel provides three-stage blast resistance against multiple explosions, leveraging its composite structural qualities, including bending resistance, catenary resistance, and sacrificial resistance, which are achieved through the contained fracture and plastification of its material components. This study introduces the principle of "Design for Multiple Intrinsic Resistance" (DeMIR) and discusses the results of blast load tests performed on the designed panels, involving four separate explosions generated by C4 explosives.

**Key words:**
**high-performance concrete, prefabrication, composite design, intrinsic resistance, blast resistance, explosives**

Prethodno priopćenje

Niyazi Özgür Bezgin

## Projektiranje predgotovljenih prijenosnih spregnutih betonskih ploča otpornih na eksploziju

Ovaj rad predstavlja pristup projektiranju za predgotovljene spregnute betonske ploče debljine 50 mm koje mogu izdržati tlak uslijed eksplozije nastao upotrebom eksploziva tipa C4 koji djeluje na njihove površine. Spregnuta ploča sastoji se od betonske jezgre visoke čvrstoće koja je spregnuta i postavljena između dviju čeličnih ploča. Projektirana ploča pruža trostupanjsku otpornost na višestruke eksplozije, iskorištavajući svoja konstrukcijska spregnuta svojstva, uključujući otpornost na savijanje, otpornost nastalog oblika lančanice i iskorištavanje koncepta "žrtvovanog" elementa, koji se postiže ograničenim lomom i plastificiranjem njegovih sastavnih dijelova. Ovo istraživanje uvodi načelo "Projekt za višestruku intrinzičnu otpornost" (DeMIR) i raspravlja o rezultatima ispitivanja opterećenja izazvanima eksplozijom izvedenima na projektiranim pločama, uključujući četiri odvojene eksplozije prouzročene eksplozivima C4.

**Ključne riječi:**
**beton visoke čvrstoće, predgotovljenost, spregnute konstrukcije, intrinzična otpornost, otpornost na eksploziju, eksplozivi**

## 1. Introduction

Explosives can serve beneficial purposes depending on their intended use. For instance, blasting rocks is common in mining and civil engineering construction. However, explosives are also employed in acts of violence and terror, where the aggressor seeks to harm civilians and military personnel. Civil engineering structures typically lack resistance to explosions, as blast loads are not included in the standard set of loads that these structures are designed to withstand. However, certain civil structures-such as embassies, security posts, transportation hubs, and financial buildings-require resistance to explosive pressures [1].

Designing structural resistance against explosives is a critical task that may involve one or more resistance qualities of the structure. For example, a thick and heavily reinforced concrete wall can be engineered to withstand explosions [2, 3]. Such a wall may remain intact under the blast pressures generated by specific quantities of explosives detonated at a particular distance. However, damage will ultimately occur if the detonation distance, amount of explosive, or type of explosive exceeds certain thresholds. In these scenarios, the wall's integrity is compromised, leading to pulverisation of its concrete elements and exposure of the reinforcing steel [4, 5]. Consequently, the structural resistance offered by the wall's bending strength and toughness is surpassed, resulting in its failure. This reaction can amplify the explosion's effects, as fragmented material from the wall may act as projectiles, causing further damage to the very individuals the structure was meant to protect. Therefore, a design approach that confines structural resistance within a composite body can be advantageous. This design can allow the structure to respond to explosions in a controlled manner, with the energy-absorbing elements confined within a framework of high tensile capability [6]. Following the depletion of the blast resistance of a wall, if the wall design does not prevent breaching of the wall fenestration, blast pressures can penetrate the protected area through the fragmented structure [7].

To improve the wall's resistance to the higher pressures generated by larger explosions, the security zone around the wall can be expanded to keep potential threats at a greater distance, or a thicker wall with heavier reinforcement can be constructed [8, 9]. However, enhancing one aspect of a structural element's design by adding more materials and increasing its weight to withstand greater blast pressures may not be the most desirable course of action. Increasing security at the expense of higher construction costs and reduced structural resilience is not an optimal solution. Design strategies for addressing explosions are typically categorised as containment, segregation, or prevention [10]. The context in which explosions occur-whether in closed structures or open air-also significantly influences the intensity of the blast pressure [11-13]. This study focuses on explosions occurring in open air, while the prevention of such explosions falls outside its scope. Containment refers to providing complete resistance against explosions, whereas segregation involves the controlled dissipation, diversion, or avoidance of explosive pressures. This study aligns with the categories of containment and segregation.

This study proposes a design approach for defensive structures called 'Design for Multiple Intrinsic Resistance [DeMIR].' This approach is grounded in the understanding that one form of structural resistance can succeed another upon its depletion or can manifest simultaneously. For instance, the design of a reinforced concrete panel necessitates establishing resistance against the bending moments created by imposed loads. Once the panel's bending strength is exceeded, it fails, and no additional support is available. In the event of an explosion, the panel material may disintegrate as it absorbs the explosive energy. If the explosive energy exceeds what can be absorbed through the disintegration of the concrete, the resisting structure can be compromised, and it will be unable to provide further resistance. However, structural design can exhibit various qualities through the material's characteristics and shape. For example, a framed reinforced concrete wall not only resists compressive, tensile, bending, and shear stresses, but it can also absorb energy through fracture enhancement under confined conditions following the depletion of its bending capacity.

This study investigates the design possibilities for a blast-resistant composite wall. This wall offers multiple forms of resistance, including bending resistance as a reinforced concrete plate with steel fibers, tensile resistance as a steel catenary integrated into the composite design through the steel plates, and energy-absorbing resistance achieved through concrete fracture as confined granular material between the steel plates, as well as tensile rupture of the steel plates. The following sections present the prefabricated design philosophy for blast-resistant composite panels, followed by their structural design. The designed panels were tested under actual blast loads at a military facility under open-air conditions. Notably, the explosion tests were not conducted indoors, allowing for effective blast pressure magnifications and reflective pressures. The panels were subjected to four explosions created using 1 kg of C4. The production sequences of the panels were documented, as they were manufactured in a civilian factory. However, photographic documentation of the tested panels was carried out by military personnel under stringent regulations. The detonation pressures were estimated using an in-house-developed numerical analysis program, calibrated with actual detonation pressure data exclusively owned by the military, details of which cannot be disclosed. Following the final detonation, the authors visually examined the panels. The requested photographs were taken by personnel, some of which were disclosed later and authorised for use in this study.

## 2. Principle of 'design for multiple intrinsic resistances (DeMIR)'

The fundamental design of the blast-resistant prefabricated concrete panels is based on the principle of DeMIR. This approach leverages the inherent strengths of the materials and

the mechanical behaviors facilitated by the structural design. For the designed composite panel, the initial resistance mechanism is the bending strength, which measures 100 cm in width, 250 cm in height, and 5 cm in thickness. A composite design was achieved by incorporating 46 mm of high-performance concrete between two 2 mm thick EN1993-1-1, S355 grade steel plates, with a yield strength $f_y$ = 355 MPa and ultimate tensile strength $f_u$ = 490 MPa. Each steel plate was conceptualised with 30 mm long shear studs, having a diameter of 6 mm, made from S420 grade reinforcing steel and welded to the steel plates with a spacing of 250 mm center-to-center along the 100 cm width of the panel. The designed concrete material, which will be detailed in the next section, was placed atop one steel plate at the specified thickness and subsequently covered by a second steel plate, thus forming the composite panel. Depending on the explosion magnitude, one or more composite panels can be utilised to create walls with thickness values in multiples of 5 cm. This multilayered design aims to facilitate recovery after an attack by simply unbolting the damaged panel from its frame and replacing it with a new prefabricated composite panel.

While the bending resistance offered by the composite panel is limited, once this bending resistance is depleted, the external steel plates begin to function as catenaries between the panel's support points, resisting tension. Consequently, the panels can still provide resistance to attacks, albeit through different mechanisms. Furthermore, the steel plates contribute additional resistance due to their shear and tensile strengths, which can manifest as punctures and tears resulting from attacks. The steel plates also confine the concrete, which may no longer be intact. Fragmented and disintegrated concrete confined by the steel plates can still resist explosions and bullet impacts through particle disintegration and shear and friction interlocking. In essence, the composite prefabricated panel exhibits three distinct modes of resistance that persist until complete failure occurs. The final resistive capacity of the composite panel is similar to that of the sandbag.

Figures 1a, 1b, and 1c illustrate the distinctive sequential resistance phases of the composite panel. The three phases of multiple intrinsic resistances for this panel are as follows:

- The bending strength of the composite panel is initially manifested.
- Following the depletion of bending strength, the tensile strength of the steel plates becomes active.
- When the steel plates develop local plastic hinges and the concrete core disintegrates, the remaining catenary strength of the composite panel, the energy absorption capacity of the concrete core situated between the plates, and the local tensile rupture of the steel plates are all engaged.

## 3. Design of high-strength concrete material for the prefabricated panel

The prefabricated composite panel was developed using high-performance concrete reinforced with 9 mm long steel fibers. The enhanced fracture energy associated with higher concrete strength grades has been shown to improve the energy absorption capacity against blast loads [14-18]. The characteristics of concrete formulated with binding mortar are critical for effective energy absorption [19]. However, this design necessitates sufficient workability of the concrete for proper placement. Therefore, trial mix designs were implemented to achieve the highest concrete strength while ensuring ease of placement. A design slump of 4 cm was specified to provide adequate workability for manual concrete placement using trowels within the formwork, which also acted as structural support for composite action.

**Table 1. Design content of the fifth concrete mixture (T5)**

| Material | Density [kg/m³] | Mass in 1 m³ concrete [kg/m³] |
|---|---|---|
| CEM I 52.5R | 3,130 | 376 |
| Silica fume | 2,200 | 33 |
| Type F – Fly ash | 2,120 | 131 |
| Aggregate | 2,700 | 783 |
| Sand | 2,600 | 1,066 |
| Plasticiser | 1,030 | 15 |
| Steel fibers | 7,800 | 15 |
| Water | 1,000 | 83 |
| **Total** | - | **2,503** |

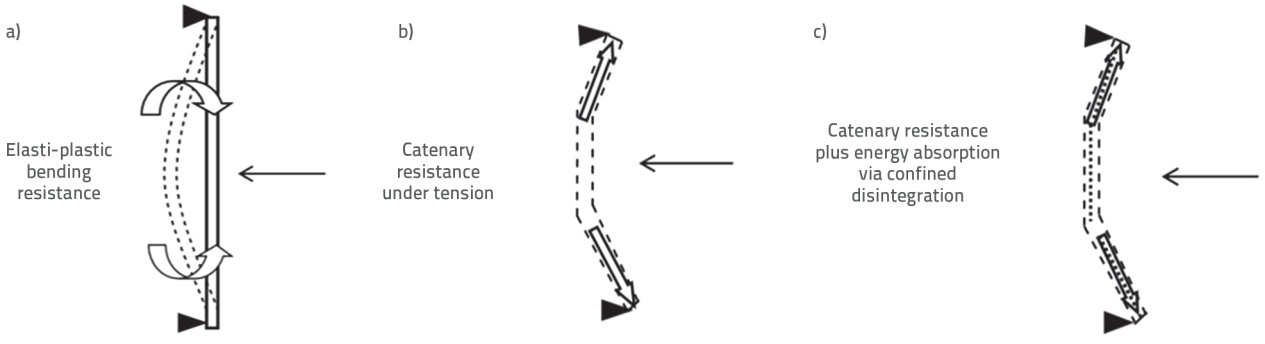


**Figure 1. Design for Multiple Intrinsic Resistance (DeMIR) mechanism of prefabricated composite plate: a) Elastic and plastic bending resistance; b) Catenary resistance under tension; c) Catenary resistance, and confined granular resistance under fracture, tensile steel rupture**

Varying proportions of the materials outlined in Table 1 were utilised to create five distinct mixture designs. Compressive strength tests were conducted on cubes with 10 cm long edges, and the results are illustrated in Figure 2. The design mixture from the fifth trial (T5) was chosen for the production of the prefabricated panels, with the contents detailed in Table 1. The 28-day strength of the cubic sample was measured at $f_{cube}$ = 122 MPa.

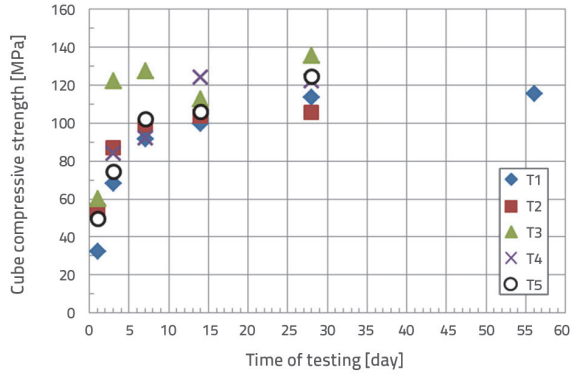


**Figure 2. Compressive strength values of cube samples obtained from five different mix designs**

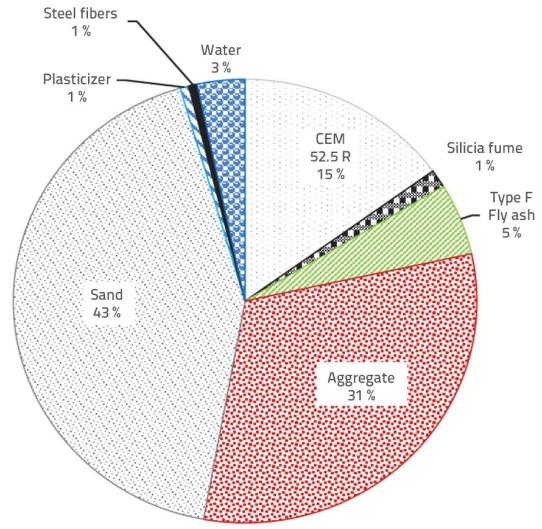


**Figure 3. Mass percentages of the constituents of the T5 concrete mixture**

The T5 mix design provided the highest strength, optimal workability, and the lowest cost using the selected design materials. The mass percentages of the concrete constituents are illustrated in Figure 3. Following the specifications of the design mixture, compressive strength tests were conducted on cylindrical samples measuring 15 cm in diameter and 30 cm in height, with results displayed in Figure 4a. Figure 4b presents the slump test results for mixture T5. Due to the capacity limitations of the force-controlled hydraulic testing device, a compressive strength test could not be performed on the 28-day-old cylindrical samples. However, the result of the 14-day compressive strength test was $f_{cyl.,14\ days}$ = 102 MPa.

A proprietary polycarboxylic-ether-based plasticiser was used in the mixture. The steel fibres had diameters ranging from 0.18 to 0.23 mm and lengths of 13 ± 1 mm. The basalt aggregates used varied in size from 5 to 13 mm. The water-to-cement ratio was set at 0.22, with a plasticiser-to-water ratio of 0.18. Angular mountain sand measuring between 0.5 mm and 2 mm was utilised. The mixing sequence lasted approximately 15 min in a high-shear mixer, starting with the saturated dry surface aggregate combined with silica fume, followed by the addition of sand and 15 % of the design water content. The remaining 85 % of the water content, along with the full amount of plasticiser, cement, fly ash, and steel fibres, was then added.

The concrete strength determined from the cylindrical samples is representative of unconfined concrete for standard reinforced concrete design. The thickness of the confined concrete between the composite plates was 46 mm. Given this thickness and its confinement state between the steel plates, the compressive strength of the concrete at 28 days, which was measured at 122 MPa based on the 100 mm thick cube samples presented in Figure 2, can be applied to define the compressive strength for this specific design of composite panels. However, the author opted to use the 14-day cylinder strength of the composite material, recorded at 102 MPa, to estimate the bending strength of the composite panel. This decision was made to avoid overestimating the mechanical bending strength by forgoing any beneficial contributions of the particular composite plate design, thus resulting in a conservative estimate anticipated to be lower than the actual strength observed during testing.

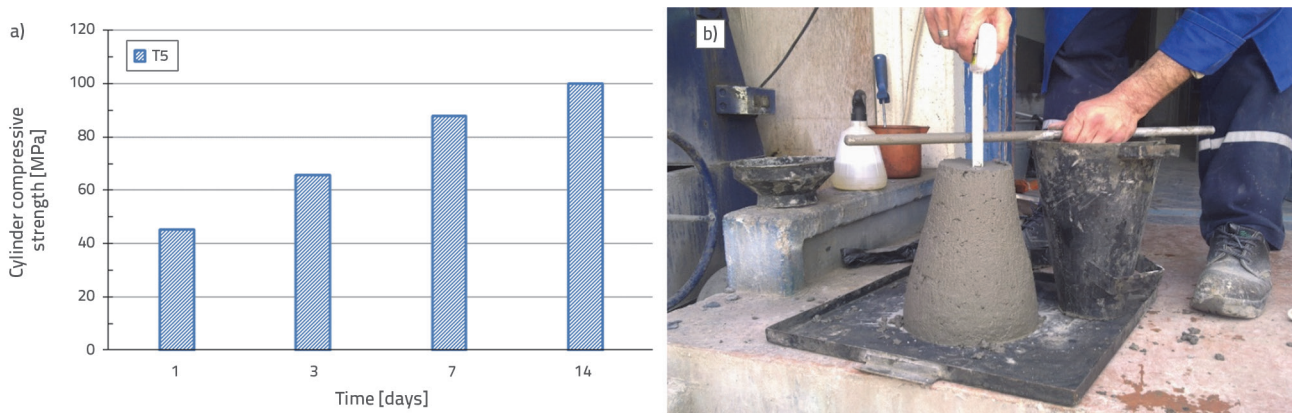


**Figure 4. a) Compressive strength values of a set of cylindrical samples obtained from the T5 mixture; b) Slump cone test of the T5 mix design showing the 4 cm slump**

## 4. Measurement of hydration temperatures

Figure 5 presents the temperature values recorded on the surface and at the centre of the cylindrical samples using concrete thermometers. The sample panels in this study were cured with heat under thermally insulated covers. The literature indicates that the specific heat of concrete ranges from c = 750 J/kg·K° to 1000 J/kg·K° [20, 21]. Given the low water-cement ratio of the design mixture and the presence of steel fibres, the lower-end value was selected to estimate the heat generated by the panels. The designed concrete had a density of d = 2,503 kg/m³. The panel contained approximately 0.115 m³ of concrete with a mass of 288 kg. Therefore, for every temperature increase above the ambient temperature, the heat energy generated by the panel can be evaluated using Eq. (1):

$$Q = m \cdot c \cdot \Delta T = 288 \cdot 750 \cdot 1 = 216{,}00 \text{ J} \quad (1)$$

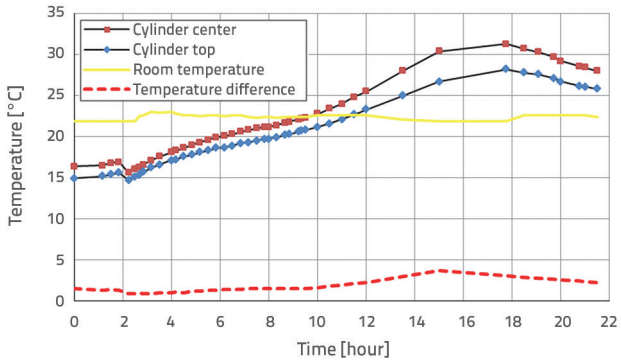


**Figure 5. Evolution of heat from cement hydration and measured temperatures**

The self-sufficiency of the heat generated from hydration for the curing of concrete is a design objective, enabling the production of composite panels without any additional curing arrangements that may be unavailable in remote locations. The amount of heat energy generated by each panel is substantial. If the heat produced during the hydration process can be retained with appropriate insulation, panel fabrication can commence without supplementary curing needs, which would be particularly advantageous in remote geographical areas where the ideal curing setup expected in a factory might not be feasible [16]. Each panel was fully wrapped in thick transparent plastic sheets and allowed to cure for 36 hours before being lifted and stacked until the tests began. The compressive strength of the designed concrete at 36 h, based on a compression test on the cylindrical sample, was 20 MPa, providing adequate strength for the panels to resist bending and shear effects due to their self-weight during transport and to prevent detachment of the plates from the core concrete of the composite panels.

## 5. Conceptualisation of composite panel design

The pre-fabricated composite panels were designed to withstand a range of explosive threats, including hand grenades, improvised explosive devices (IEDs), surface detonations of 1 kg of C4, and potential attacks involving concealed, larger amounts of explosives, such as TNT or C4, which may not be easily placed by hand but could be transported to a location within 5 m of the target by vehicles or other means. This design makes the proposed blast-resistant composite panels suitable for both military and civilian applications. For the anticipated explosive conditions at a 5-meter distance, the design accounted for 10 kg of C4, resulting in a peak pressure of 150 kN/m² [17].
To facilitate rapid construction, the panels were designed to harness the self-generated heat from hydration, enabling them to quickly gain the necessary early strength. The initial concept involved creating 50 mm thick composite panels, composed of 2 mm thick steel plates and a 46 mm concrete core. Each panel was designed to resist a static pressure of 50 kN/m², necessitating the use of three composite panels in sequence to withstand a peak pressure of 150 kN/m². The steel plates, equipped with welded shear studs, served dual purposes: as formwork during concrete placement and as external steel reinforcement to counter bending stresses, tensile catenary stresses, and to contain fractured concrete, enhancing energy absorption from blasts. Through the shear studs, the steel plates were mechanically bonded to the concrete core, functioning as external reinforcement for the concrete until failure. The overarching aim was to demonstrate that the external mechanical bond between the plates and concrete core could emulate the behaviour of an internally reinforced concrete plate. For this purpose, shear studs were strategically selected and spaced to sustain the necessary shear flow between the

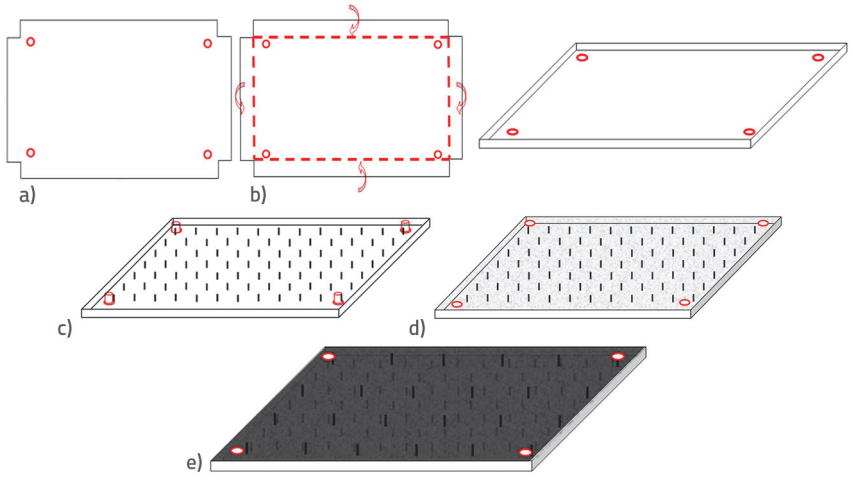


**Figure 6. Production sequence sketch for the prefabricated composite panels: a), b) Bending of the specially shaped 2 mm thick steel plate; c) plate with welded shear studs and corn; d) placement of the concrete; e) Placement of the top plate with welded shear studs**

steel plates and the concrete core.

Figures 6a and 6b illustrate the preparation of the base plate, which acts as the formwork for the concrete placed on top and serves as the tensile/compressive reinforcement for the composite section. The marked circles represent pre-drilled holes intended for securing the composite panels to their supporting frames, as discussed in subsequent sections. Figure 6c shows the welded shear studs, with 6 mm diameter and 30 mm length, spaced at 25 cm centre-to-centre along the plate's 100 cm width. These studs were positioned 12.5 cm from the edges of the steel plates. The shear studs on the top plate were offset by 12.5 cm from those on the bottom plate to avoid interference. The studs were welded to the plates, and bolt holes were drilled, as shown in Figure 6a, before moving to the configuration illustrated in Figure 6c. Concrete was placed as shown in Figure 6d, and the top plate, with welded studs and attachment holes, was positioned on top of the concrete, as shown in Figure 6e. The shear studs from both the top and bottom plates penetrated the fresh concrete, and the composite panel was then covered and allowed to cure for 36 h. With adequate coverage, the concrete was able to gain sufficient strength from its own heat of hydration and retained moisture, allowing the 50 mm thick composite panels to be lifted and stored.

Once the conceptual basis was established, the work progressed with the estimation of the bending strength of the conceptualised panel and determination of its shear-stud requirements.

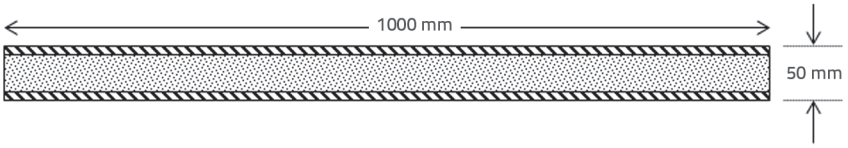


**Figure 7. Sketch of the width of the composite panel showing the two steel plates and the concrete core (not to scale, shear studs not shown)**

## 6. Estimation of the design bending moment and the design for the shear transfer between the concrete core and the steel plates

As outlined in the previous section, each composite panel was initially designed to withstand a blast pressure of 50 kN/m$^2$, with any surplus capacity left to be confirmed through bending tests. Figure 7 illustrates a not-to-scale cross-section of the composite panel. A 46 mm thick concrete core was enclosed between two steel plates, each measuring approximately 2 mm ± 0.5 mm in thickness. Welded shear studs with a 6 mm diameter were attached to the steel plates (not shown in the figure). These studs, with a 4 mm thick perimetric weld and a weld shear strength of $f_w$ = 250 MPa, penetrated 30 mm into the concrete core. The studs were placed at regular centre-to-centre intervals along the length and width of the steel plates to ensure effective shear transfer.

Before the actual blast-load tests, the plates were designed to withstand a peak pressure of $p_s$ = 150 kN/m$^2$. Eq. (2) calculates the highest bending moment generated by this pressure along a simply supported set of plates, bearing on 150 mm wide end beams with a clear span of 2.2 m between the bearing beams. This calculation was based on using three composite panels, each designed to carry 1/3$^{rd}$ of the peak pressure of 150 kN/m$^2$ and 1/3$^{rd}$ of the moment, which is presented in Eq. (2):

$$M = (150 \cdot 1 \cdot 2{,}2^2)/8 = 91 \text{ kN.m} \quad (2)$$

The mechanical design of the composite plate deviates from conventional reinforced concrete approaches. Here, the composite plate functions as an externally reinforced concrete structure. In this design, the steel plate on the compression side is mechanically bonded but may buckle when the bending strength of the composite plate reaches its limit. As a result, the theoretical capacity of the composite plate is conservatively estimated by excluding the compressive side steel plate's contribution and limiting the tensile strength of the tensile side steel plate to its yield stress, $f_y$ = 355 MPa. Figure 8a shows the relationship between mean compressive stresses and varying strains in concrete cylindrical specimens [23]. For typical concrete up to C50 grade, approximately 50 % of the design strength lies within the linear and elastic behaviour range. In contrast, C100 grade concrete exhibits nearly linear stress-strain behaviour up to around 80 % of its compressive strength, making it a suitable choice for high-stress applications. Figure 8b illustrates

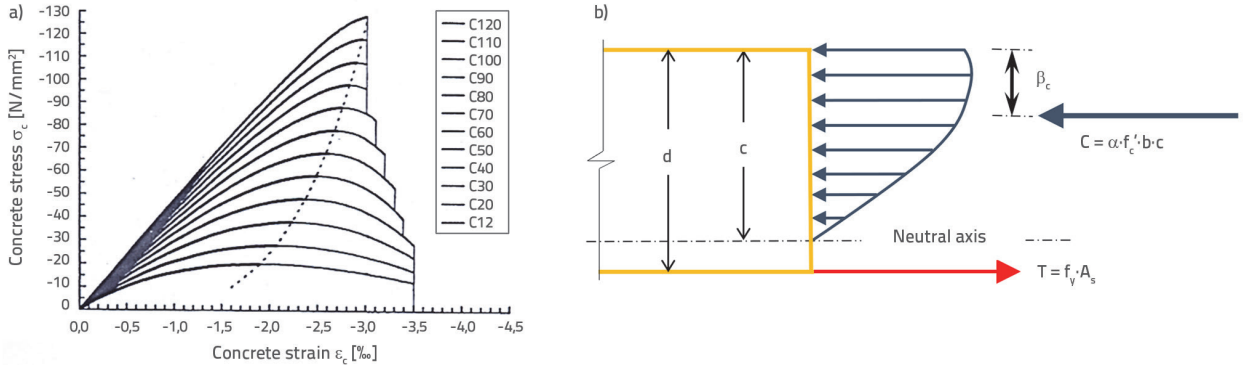


**Figure 8. a) Stress–strain curves for various concrete strength grades [23]; b) Sketch of the distribution of compressive concrete and tensile steel stresses within the structural cross section**

the stress distribution within the composite panel cross-section, where "b" is the width of the composte plate, "c" is the depth of the compressive stress block, and "d" is the distance from the top of the composite plate to the centroid of the tensile steel plate. This sketch omits the contribution of the compressive steel plate. The average compressive stress within the compressive region of the concrete and the location of the resultant compressive force is represented by the coefficients $\alpha$ and $\beta$, respectively [24]. The coefficients $\beta = 0.56$ and $\alpha = 0.325$ are used to characterise the stress distribution within the compressive region of C100 grade concrete.

Eq. (3) shows the tensile steel ratio of the composite plate. Using Eq. (4), the nominal bending strength of the composite plate is estimated as Mn = 30 kN.m in Eq. (5). Based on a clear bending span of L = 2.2 m, Eq. (6) presents the equivalent distributed pressure on the panel that generates the highest bending moment of $w_n$ = 53 kN/m² that generates the highest bending moment $M_n$=32 kN.m.

$$\rho = \frac{A_s}{b \cdot d} = \frac{20}{100 \cdot 4{,}7} = 0{,}0425 \quad (3)$$

$$M_n = \rho \cdot f_y \cdot b \cdot d^2 \cdot \left(1 - \frac{\beta \cdot f_y \cdot \rho}{\alpha \cdot f_c'}\right) \quad (4)$$

$$M_n = 0{,}0425 \cdot 35500 \cdot 100 \cdot 4.7^2 \left(1 - \frac{0{,}325 \cdot 35500 \cdot 0{,}0425}{0{,}56 \cdot 10200}\right) = 32 \text{ kNm} \quad (5)$$

$$w_n = \frac{8 \cdot M_n}{L^2} \rightarrow w_n = 53 \text{ kN/m}^2 \quad (6)$$

The highest shear force exerted on the plate, $V_{maks}$, under the action of wn is given by Eq. (7), where "b" is the width of the plate and b = 1 m and the clear span L = 2.2 m.

$$V_{max} = \frac{w_n \cdot b \cdot L}{2} = \frac{53 \cdot 1 \cdot 2{,}2}{2} = 58 \text{ kN} \quad (7)$$

The conservatively estimated nominal bending strength capacity of the composite plate and the corresponding value of the distributed pressure did not consider the effects of the compressive steel plate or the confined compressive strength of the concrete. The contribution of the compressive steel was omitted because the exact behaviour of the composite plate under bending was unknown prior to the static bending tests. Although the steel plate under compression was thought to be sufficiently bonded to the concrete, its exact behaviour under actual loading conditions is unknown. Therefore, any excess bending capacity, which was considered to be present in addition to the nominal bending capacity presented in Eq. (9), was omitted.

## 7. Design for the transfer of shear between the concrete core and steel plates

The design of the shear studs is a critical aspect of the proposed composite design. The shear studs not only mechanically bond the steel plates to the core concrete, providing a load path for the transfer of shear stresses to realise the tensile strength of the steel plates, but also provide lateral bracing. This bracing prevents the steel plate under compression, when the composite plates are bent, from buckling outwards up to its point of failure under bending. Steel plates are present and remain in contact with the concrete at all resistance stages of the composite panel. Shear studs welded onto the plates facilitate stress transfer during bending. To determine the amount of shear stress transferred to the concrete core of the composite plate, the properties of the composite cross-section were assessed. Figure 9 shows the cross section of a 100 cm wide panel with 4.6 cm thick concrete and 2 mm-thick steel plates. The elastic modulus of steel is $E_s$ = 210.000 MPa, and the elasticity modulus of C100 grade concrete is Ec = 43,895 MPa, with a modular ratio of $\eta = E_s/E_c = 4{,}78$ [23]. Eq.s (8) and (9) present the composite moment of inertia of the plate and the static moment of one steel plate with respect to the centre of gravity of the section, which coincides with its geometric centre in this case.

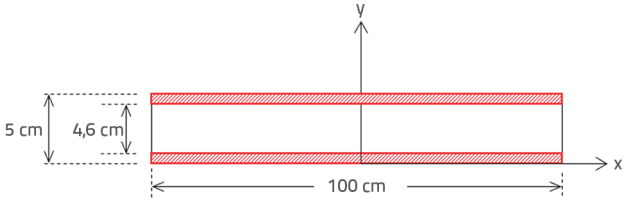


**Figure 9. Cross-section of the composite plate (not scaled, shear studs not shown)**

$$I_{composite} = \frac{4{,}6^3 \cdot 100}{12} + 2 * \frac{0{,}2^3 \cdot 100 \cdot 4{,}78}{12} + 2 \cdot 0{,}2 \cdot 4{,}78 \cdot 2{,}4^2 = 1{,}913 \text{ cm}^4 \quad (8)$$

$$Q = 0{,}2 \cdot 100 \cdot 4{,}78 \cdot 2{,}4 = 229 \text{ cm}^3 \quad (9)$$

Composite panels were designed for a distributed pressure of 50 kN/m² along their clear 2.2 m span. The highest shear occurred near the support points, reducing linearly to zero at the midspan of the beam under distributed forces. The highest shear stress that must be transferred between the steel plate and the concrete core is given in Eq. (10), where "V" is the shear force to be transferred, estimated as V = 58 kN in Eq. (7), and "t" is the width of the shear area.

$$\tau = \frac{V \cdot Q}{I \cdot t} = \frac{58 \cdot 229}{1913 \cdot 100} = 0{,}069 \text{ kN/cm}^2 = 0{,}69 \text{ MPa} \quad (10)$$

Along a width of 100 cm, four studs were welded at 25 cm intervals from centre to centre. Each row of studs was welded with a spacing of 25 cm along the length of the steel plate, giving each stud a tributary area of $A_t$ = 25 cm · 25 cm = 625 cm². Based on the transferred shear stress shown in Eq. (10) and the calculated At, Eq. (11) presents the shear force "S" that must be transferred by each shear stud.

$$S = \tau \cdot A_t = 0{,}69 \cdot 625 \cdot 100 = 43{,}125 \text{ N} \quad (11)$$

Shear studs transfer shear through bearing onto the concrete core. The shear studs were made from S420 grade steel

reinforcement bars, with a yield strength of $f_y$ = 420 MPa and diameter D = 6 mm, cut to length, resulting in a length-to-diameter ratio of L/D = 5.83. The deformation of the shear studs due to bending was considered negligible. Figure 10a shows a sketch of the shear stud under a shear force (S) acting on its left side, resisted by the pressure bulb formed along its right side. The shear stud was welded to the steel plate around its circumference and bottom, as shown in Figure 10b. The tensile strength of the weld was $f_E$ = 420 MPa, the shear strength was $f_s = 0{,}7\ f_E$ = 294 MPa, and the length of the weld leg was 4 mm.

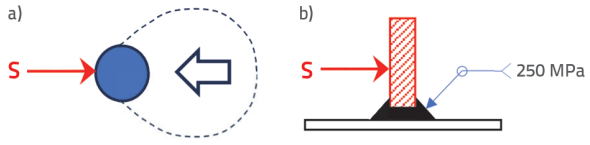


**Figure 10. a) Plan view of the shear stud bearing onto the concrete under the shear force (S); b) Profile view of the shear stud welded onto the steel plate**

The bearing area of the shear stud on the concrete core was estimated to be $A_b = 2 \times D \times L = 360\ mm^2$, considering the formation of the bearing stress bulb behind the shear stud. Therefore, each stud that resists the shear force, as presented in Eq. (12), produces the bearing stress "$f_b$" in the concrete, given by Eq. (12), which is lower than the nominal compressive strength of the concrete based on its cube strength $f_{kocka}$ = 122 MPa.

$$f_b = (S/A_b) = (43{,}125/360) = 120\ MPa < 122\ MPa \quad (12)$$

The transfer of shear from the plate to the stud and concrete core requires welding to the steel plate. With a weld leg size of 4 mm, the weld area is $A_w = 154\ mm^2$, and the shear stress on the weld is expressed by Eq. (13), which is lower than the shear strength.

$$F_w = (S/A_w) = (43{,}125/153) = 281\ MPa < 294\ MPa \quad (13)$$

The conceptual design of the prefabricated composite panel was based on the strength parameters of the materials used and considerations of the panel's mechanical response under bending. The next stage involved producing these samples and performing static and blast loading tests. During the production phase, certain modifications were applied to the composite plates regarding shear transfer. The hypothetical use of 6 mm diameter and 30 mm long shear studs proved more difficult to construct in the steel shop when compared to their seemingly simple suggestion on paper.

According to the design, each plate required 40 shear studs, meaning that each composite panel with two steel plates required the individual welding of 80 shear studs. Unless the welding was performed automatically-where each stud, precisely cut to dimensions, acted as the electrode (which was not the case)-manual welding of these short shear studs proved difficult for the technicians and workers in the steel shop. Manual welding could not guarantee the quality of the shear stud connections.

Under time constraints for producing samples for the blast loading tests at military grounds, the author revised the design and proposed a bolted version of the composite panels. In this version, most of the shear studs were omitted and replaced with 46 mm high cylinders, featuring external and internal diameters of 24 mm and 20 mm, respectively. These cylinders were spot welded onto the steel plates with predrilled 20 mm diameter holes, allowing bolts to secure the composite panels for the tests. Initially, blast testing was conducted on three composite panels with a total thickness of 15 cm. Following this revision, we decided to test two composite panels with a total thickness of 10 cm. The mechanical strength of each composite panel and the final composition of the two bolted panels were expected to exceed those anticipated from the design estimations. Consequently, the decision was made to omit the shear studs along the 90 cm lengths at both the top and bottom of the panels and replace them with cylindrical attachments welded around the predrilled holes in the steel plates. These attachments provided space for the placement of bolts securing the two composite plates for blast testing. Figure 11 illustrates a plan sketch of the steel plates reflecting the changes made for production. However, the author insisted on the inclusion of eight shear studs, each with a diameter of 6 mm and a length of 30 mm, in the middle 70 cm length of the panels to assess the performance of the shear studs under static and blast loading tests. Two rows of studs were welded at 20 cm from the centre along the 100 cm width of the panel, with a spacing of 50 cm between the two rows.

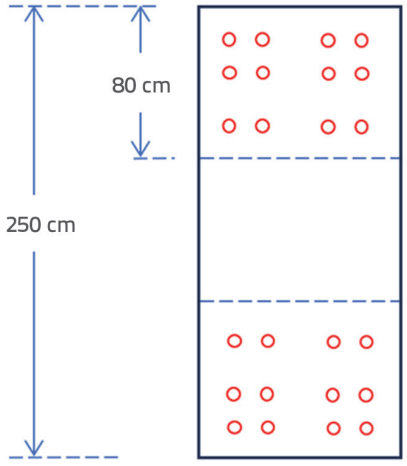


**Figure 11. Sketch of the plan view of the revised steel plate for production and testing**

## 8. Production of composite prefabricated panels

Figure 12 illustrates the production process of the composite panels. Following the placement of the first steel plate, which had its edges bent to form a cast for the concrete, highly plastic concrete was placed and spread using trowels. The concrete was evenly distributed over the steel panel, which served as formwork. The concrete possessed sufficient plasticity to retain its shape and facilitate its placement. Subsequently, the top steel plate was positioned over the concrete, sandwiching the high-performance concrete between the two shear-studded steel plates. The concrete

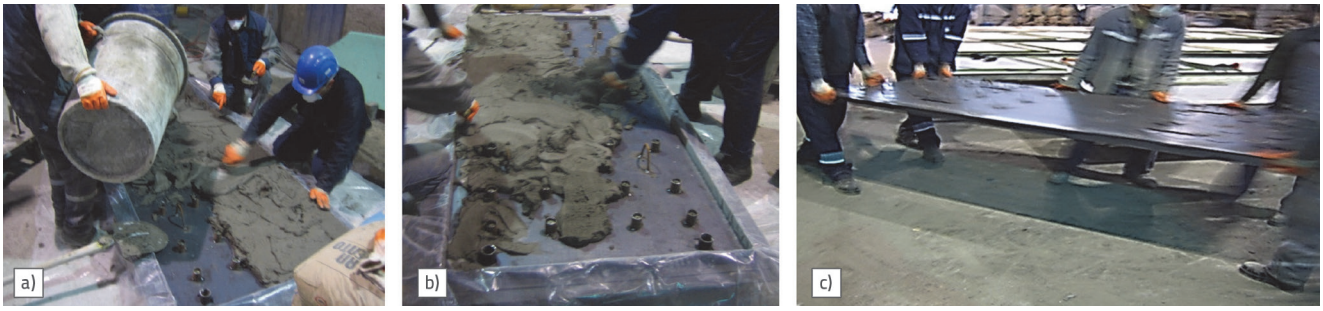


**Figure 12. Production sequence of a panel followed by its manual transport: a) concrete placement; b) spreading of concrete; c) manual transport of the finished composite concrete plate**


**Figure 13. Production sequence of a panel: a) placement; b) spreading; c) finishing**

placement and the closure of the composite panel, which had an approximate mass of 360 kg, took about 30 min with the assistance of five workers.

The cylindrical attachments shown in Figure 12 were welded around the perimeter of the circular holes cut into plates to prepare space for the bolts to attach to multiple panels. Figure 13 shows another production sequence in a cool environment where the ambient temperature was measured between 10 °C and 15 °C. The condensation fumes resulting from the heat generated by the concrete mass are shown in Figure 13a. The consistency of the concrete allows sufficient plasticity for manual placement and shape retention, which facilitates the placement of concrete.

## 9. Results of the static bending test for the composite plate

Figure 14 illustrates the moments during the static four-point bending load test conducted on a single panel measuring 250 cm in length, which rested on steel box beams of the test frame with 15 cm wide bearing widths. The test was force-based, whereby the plates were loaded by a hydraulic press until the bending resistance was reached, and the increase in load pressure, as measured from the hydraulic gauge, ceased. The welded cylindrical attachments to the plates facilitated the transfer of shear between the concrete core of the panels and the steel plates. The simply supported panel, with a clear span of L = 2.2 m, was gradually loaded at L/4 and 3L/4. The single concentrated load, 2P, applied by the hydraulic press at the middle span, was divided into two equal forces by beams supported at L/4 and 3L/4 along the panel. The panel reached its bending strength at approximately 2P = 200 kN, at which point the top compression plate buckled, followed by compression failure of the concrete core, tensile cracking, and detachment from the bottom plate under tension. Each of the concentrated forces P at L/4 and 3L/4 was 100 kN, producing the bending moment shown in Eq. (14) along the plate span between L/4 and 3L/4.

$$M = (P \cdot L/4) = (100 \cdot 2{,}2/4) = 55 \text{ kNm} \quad (14)$$

The tested bending strength of the composite panel M = 55 kN-m was significantly higher than its conservatively estimated nominal bending $M_n$ = 32 kNm shown in Eq. (5). The distributed pressure on the exposed face of the composite panel that generates the maximum bending moment M = 55 kNm is presented in Eq. (15).

$$w_n = (8 \cdot M_n/L^2) \rightarrow w_n = 91 \text{ kN/m}^2 \quad (15)$$

The panel's bending limit was reached due to local buckling of the top plate and failure of the concrete core under compression. The panel was loaded until failure at force

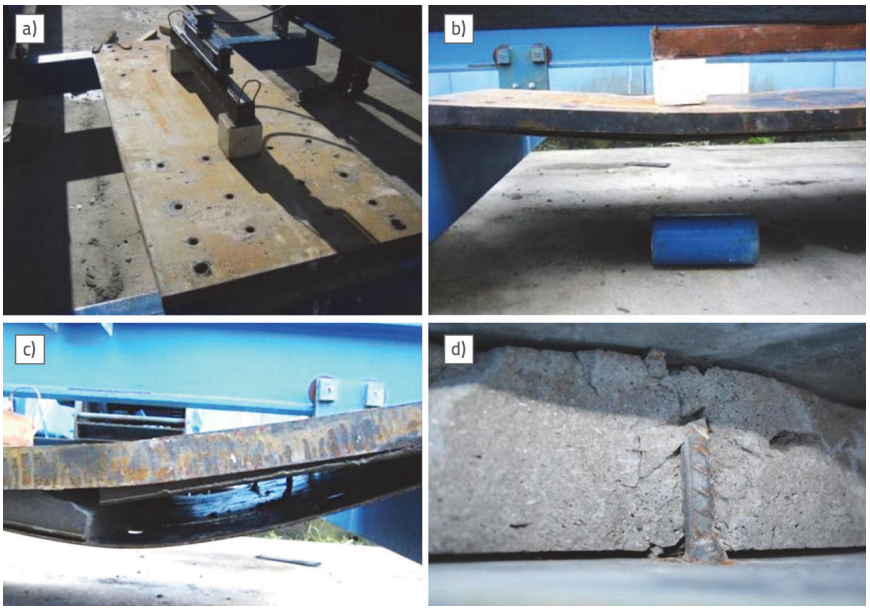


**Figure 14. Static four-point plate bending test of the composite panel: a) initial loading stage; b) local buckling of the top compression plate; c) detachment from the compression plate, crushing of the top of concrete core followed by its failure under excessive bending; d) bearing of the concrete core onto the shear stud welded on to the tensile plate**

intervals of approximately 10 kN, at a rate of around 10 s per interval. Subsequent excessive deformation led to the remaining concrete core fracturing under tension. The residual connection of the bottom plate to the concrete through the shear studs maintained the panel's integrity, and despite the bending failure, the plates remained connected to the individual pieces of concrete between them. Figure 14c depicts the panel loaded beyond the failure point, indicating the complete fracture of the concrete core. Figure 14d illustrates the shear stud bearing on the concrete and the resulting failure of the concrete due to this bearing. The bending test, conducted as a proof-of-concept, demonstrated that the plates bonded to the concrete core through shear studs functioned as a tensile support for the otherwise brittle concrete under pure bending. While the composite concrete panel could no longer resist bending, it remained supported between the plates and was still capable of providing resistance through fracture, absorbing energy under explosive attack.

Following the static test, it was determined that two panels, each with a total bending strength of 55 kNm, would provide a combined bending capacity of 110 kNm, exceeding the design bending moment of 91 kNm presented in Eq. (2). The joint action of the two composite plates bolted together was expected to further enhance their combined bending capacity beyond 91 kN-m. However, for the sake of clarity and to avoid unsupported assumptions, the resultant bolted composite behaviour of the two individual panels was not considered.

## 9. Results of full-scale blast loading tests conducted on pre-fabricated composite panels

During the second phase of the tests, conducted as a proof-of-concept for the DeMIR used in the design of the composite panels, two sets of composite panels-each comprising two panels-were transported to a military site and bolted together. Each set of panels was secured from both ends to a triangular frame made of box steel sections. One set of panels was selected for testing under blast loads, while the second set was reserved as a backup for the military. The test set was subjected to four detonations of C4 explosives, positioned at distances of 775, 275, 25, and 0 cm from the surface of the test panels to the explosives' surface. The tests commenced at 09:10 and continued until 13:30. Safety protocols mandated a 1 km standoff from the blast site both before and after the completion of the blast tests. Ambient temperatures during the testing period ranged from 10°C to 15°C. The pressures generated by the explosions occurred over the order of milliseconds; therefore, the behaviour of the panel was markedly different from that observed in the static bending load tests illustrated in Figure 13. The pressure diagrams presented in Figure 14 correspond to the explosions that occurred at d = 25, 275, and 775 cm from the panel surfaces. These diagrams are based on proprietary numerical software developed by military engineers, utilising actual explosion pressure test data. The blast pressure peaks lasted from 0.1 to 0.3 milliseconds, depending on the detonation distance. Table 1 outlines the estimated and extrapolated peak pressures at a distance of d = 0 m, which cannot be numerically calculated by the program owing to the mathematical singularity at d = 0 m.

The pressure profiles depicted in Figure 15 indicate the atmospheric pressure at sea level, which is 101.3 kPa. These profiles illustrate the development of a positive pressure

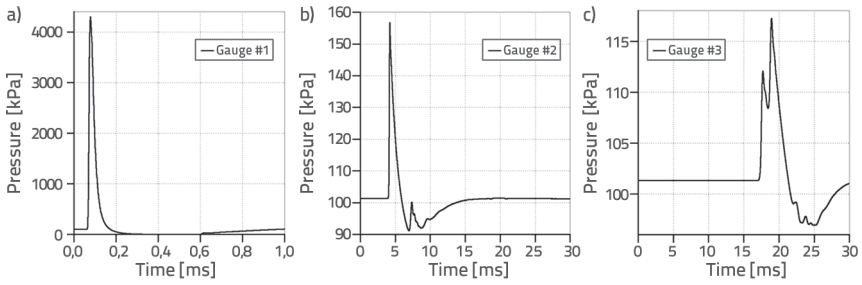


**Figure 15. Numerical explosion pressure estimates at distances: a) d = 25 cm; b) d = 275 cm; c) d = 775 cm from the surface of the composite panel, based on proprietary software**

peak, followed by a negative pressure phase relative to a reference pressure of 0. Table 2 presents the estimated and extrapolated peak blast pressures, while Figure 16 shows the variation in peak pressures with distance. The exponential curve representing this variation was fitted with an $R^2$ value of 0.95, indicating a strong correlation. This curve approaches infinity at d = 0 cm. However, despite this mathematical characteristic, it is acknowledged that a physical value for the blast pressure exists, albeit it is incalculable using the numerical procedure proposed by the program developers. Military officials suggested that the maximum pressure at d = 0 cm should be considered a minimum of 10,000 kPa.

**Table 2. Maximum estimated pressures based on proprietary numerical software and suggested maximum pressure at d = 0**

| Explosion distance (d) to the panel surface from the edge of the charge [cm] | Estimated pressures (P) and suggested pressure vat d = 0 cm [kPa] |
|---|---|
| 0 | 10,000* |
| 25 | 4180 |
| 275 | 157 |
| 775 | 117 |

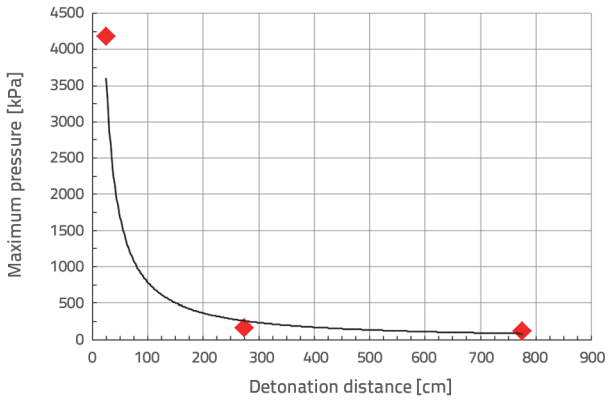


**Figure 16. Variation of numerical explosion pressure estimates with distance based on proprietary software**

The fourth explosion, at d = 0, resulted in observable damage to the panels. Figures 19b to 19f illustrate the panel damage from various angles. Figures 19b, 19c, and 19d show the crater generated within the steel plate, which measures approximately 20 cm in diameter. The top steel plate reached its plastic limit and exhibited a deformation of about 6 cm. The first plastified steel plate formed a partially spherical dome with a diameter of 20 cm and a height of 5 cm. The blast pressure penetrated both the top composite plate, which has a thickness of 5 cm, and the second composite plate of the same thickness, as depicted in

The first blast test, conducted at a distance of 775 cm from the face of the panel, had no observable effect on the panels; therefore, images from this test are not included. Figure 17.a presents the results of the second blast test, where 1 kg of C4 was positioned 275 cm from the face of the test panel. Figure 17.b depicts the condition of the panel face after the explosion. The blast did not cause any visible reactionary damage to the face or sides of the panels; instead, it resulted in blast burns on the exposed surface. Figure 18.a illustrates the placement of the same quantity of C4, this time positioned 25 cm from the surface of the test panel. Figure 18.7b shows the condition of the panel faces following the explosion. Once again, there was no visible reactionary damage to the panels; however, the blast burns were significant. Figure 19.a shows the placement of the explosive directly on the surface of the panel, which was the last explosion test conducted with the remaining available explosive. Throughout all tests, the composite plates were supported between two square box steel beams with a bearing width of 150 mm.


**Figure 17. a) C4 blast set 275 cm from the face of the panels; b) Panel face after blast showing minor blast burns but no observable structural damage**


**Figure 18. a) C4 blast placed 25 cm away from the face of the panels; b) Panel face after the explosion showing blast burns but no observable structural damage**

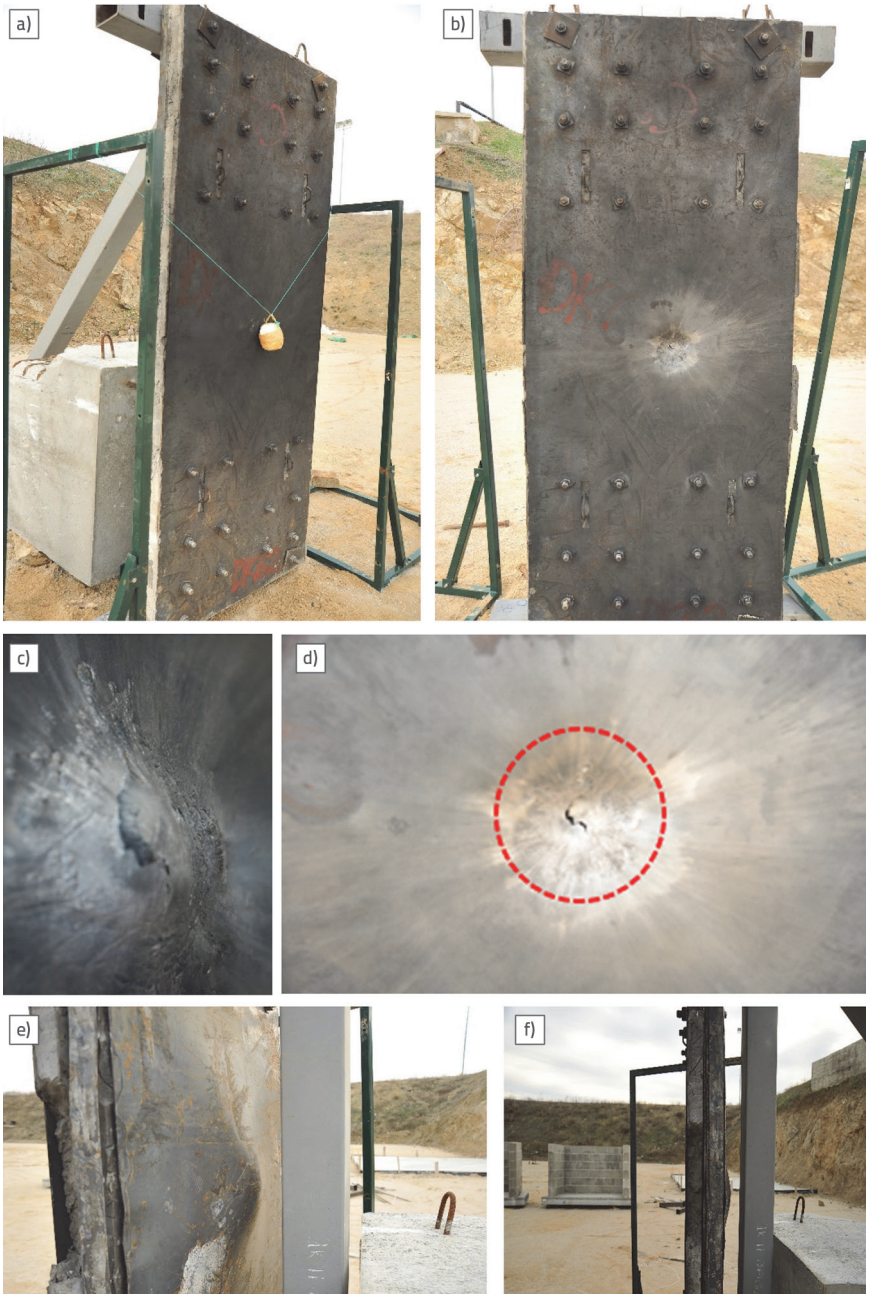


**Figure 19. a) C4 blast set 25 cm above the face of the panels; b, c, d, e, f) State of the panels after the blast showing penetration of the first panel but no penetration through the second panel**

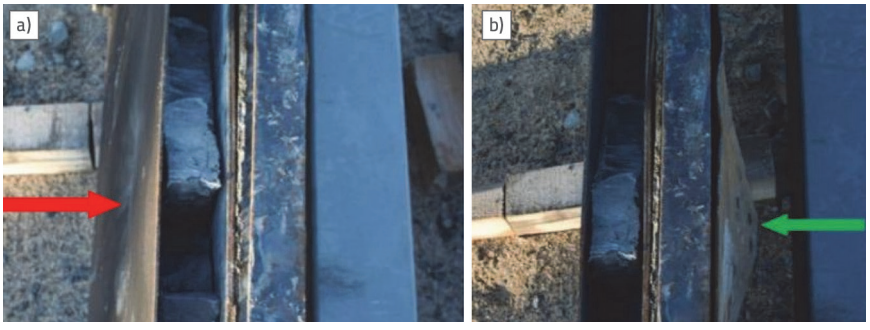


**Figure 20. a) Direction of the blast effect; b) Two composite panels provide resistance**

Figures 19e and 19f. However, the blast pressure did not penetrate the back plate of the second composite panel.

Figures 20.a and 20.b demonstrate the directions of the blast effect and the corresponding resistance to the blast effect, respectively. Figure 19.a shows the fractured concrete core as the blast pressure penetrated the concrete plate. Despite the damage, the two composite plates, with a total thickness of 10 cm, effectively prevented the complete penetration of the blast pressure, allowing the wall to remain intact. The recommended course of action following such an attack is to remove the damaged panels from the frame and bolt new panels onto the existing frame.

Figures 21.a to 21.d illustrate the fractured concrete bearing on the shear studs and the compressive failure of the concrete observed in the shear stud bearing areas within the central portion of the composite panels. The observations indicated that the duration of the blast effect was primarily resisted by the energy absorption of the concrete core due to fracture, along with the plastification and tearing of the steel plates. The plates effectively confined the concrete core, enabling the controlled disintegration of the concrete to absorb the blast energy. In Figure 21c, the shear stud is shown bent as the fractured concrete shifted sideways, while the shear stud in Figure 21d penetrated the bearing concrete. These figures demonstrate that the shear studs functioned effectively and, together with the plates, confined the concrete. Despite the concrete's fracture, this configuration provided adequate support to utilise the toughness qualities of the disintegrating concrete for energy absorption.

Figure 22 presents the interior of the central 100 cm of the first composite plate that was directly exposed to the explosion. The upper steel plate has been removed for further investigation. The pulverised concrete zone located beneath the first penetrated steel plate is depicted in Figures 22a and 22b, with a diameter of approximately 30 cm. Radial extensions of clean fracture

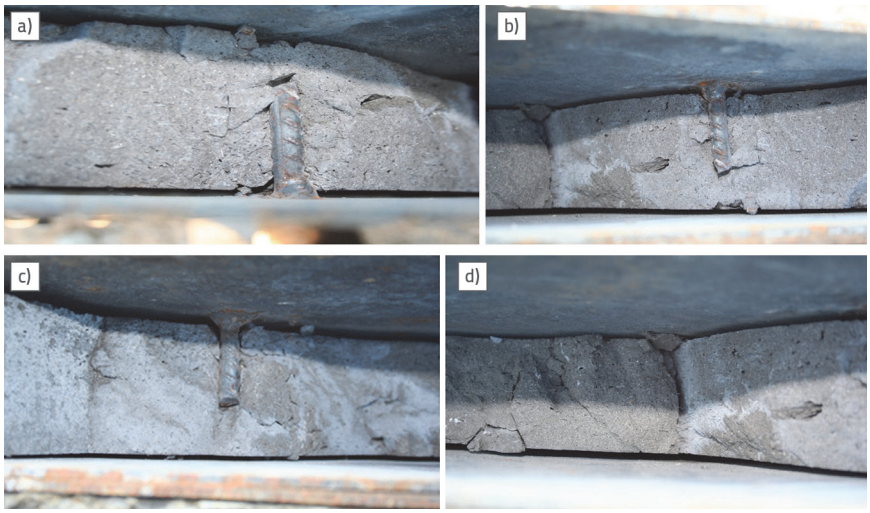


**Figure 21. Interior of the central part of the composite panel showing the concrete core, highlighting the concrete core bearing on the steel shear studs welded to the top and bottom plates, and the compressive crushing of the concrete bearing on the shear studs**

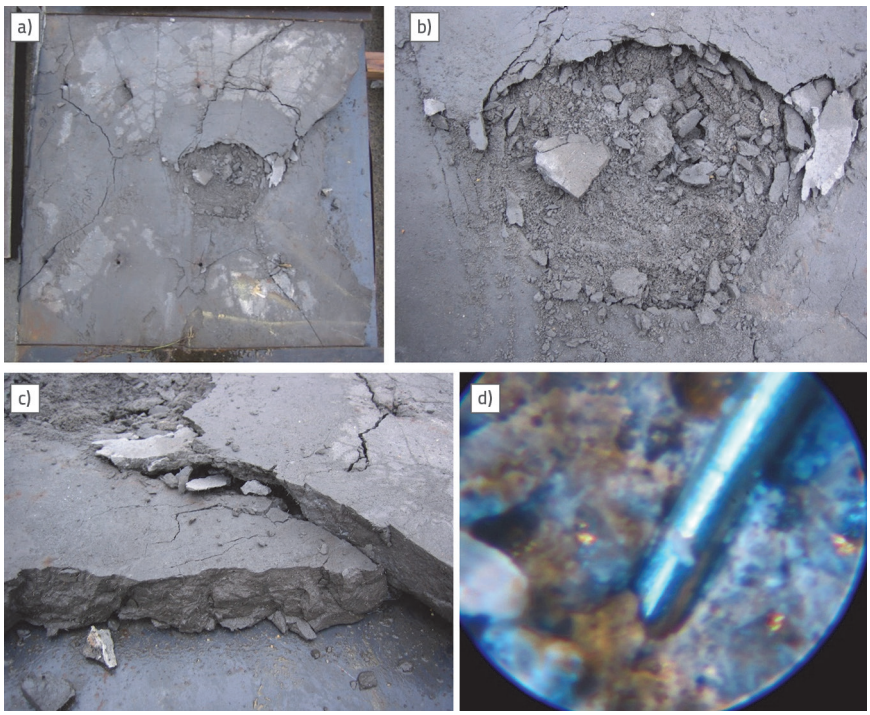


**Figure 22. a) and b) Fracture and pulverisation within the concrete inside the first composite panel directly exposed to the blast effect of 1 kg C4; c) fractured concrete between the two plates; d) x100 close-up view of a steel fibre embedded in concrete**

zones can be observed beyond the pulverised area. Figure 22c highlights the presence of steel fibres along the crack edges of the concrete pieces, while Figure 22d provides a magnified view of the concrete surface, showcasing the embedded steel fibres.

The back plates of both the first and second composite panels were separated from the frame for examination. However, due to a managerial oversight by the author, the images from this investigation were unfortunately lost as a result of digital file failure and a lack of backups. It was noted that the second steel plate at the back of the first composite panel also reached its plastic limit and exhibited a tear similar to those shown in Figures 19c and 19d, albeit with a shorter length of approximately 30 mm. The crater diameters of both the first and second steel plates of the second composite panel measured around 15 cm, with a maximum depth of approximately 4 cm. Within the concrete core of the second composite panel, the diameter of the pulverised concrete zone was about 20 cm, featuring similar, albeit shorter, radial fracture zones. The second steel plate of the second composite panel exhibited plastification as seen in Figure 19e, but the blast pressure did not penetrate through it. Consequently, the explosive energy from the 1 kg of C4 was effectively contained within the two composite panels, each with a thickness of 5 cm, resulting in concrete core fracture, along with plastification and tearing of the steel plates. The bending resistance offered by the plates to the blast pressure was not observed or instrumented. However, if bending resistance did occur, it was not the primary mode of resistance due to the very short duration of the blast pressures. The experimental setup consisted of two composite panels subjected to four consecutive blast loads, spaced approximately 40 minutes apart. The blast that impacted the face of the composite panels at d = 0 cm caused observable damage, demonstrating that the composite panels performed as expected under blast pressure and effectively absorbed energy within the confines of the steel plates.

Steel fibres embedded in concrete have proven beneficial under blast forces. An examination of the fractured pieces revealed that the fibres remained embedded and did not entirely disintegrate from the concrete. Although their relative effectiveness compared to a fibre-free concrete design was not quantified in this study, the fracture characteristics observed in the concrete cores of the composite plates indicated that the fibres supported the controlled and confined disintegration of the concrete.

## 10. Conclusions

This study focused on a series of developments and tests aimed at evaluating the effectiveness of the proposed DeMIR design principle. Developing structural resistance to blast pressure involves considerations of limited state performance. The magnitude of such loads often exceeds the elastic limits of the resisting structures, and effective resistance typically necessitates redirection or dissipation of the blast effects. Designing a structure capable of withstanding blast forces within elastic limits can be a costly endeavor and may present architectural challenges. Specifically, elastic resistance to blast forces is a significant concern for shelters or hangar structures, which are expected to remain fully intact and operational following blast attacks. Conversely, sacrificial design principles, applicable to lightweight and mobile solutions against blast forces, can offer flexibility in design performance and serviceability.

This study was initiated through a collaborative effort between the private sector and the government, with financial support from the Turkish Scientific and Technological Research Council (TUBITAK) via the TEYDEB 1501 program, which aims to foster joint scientific endeavors among the private sector, academia, and governmental bodies. Conducted in 2010, the authors sought to develop lightweight and mobile solutions for defense structures against explosive threats. The private sector involvement included a precast concrete producer with whom the author collaborated to design and develop prefabricated concrete elements. Government involvement encompassed military ground forces and the military corps of engineers. The author proposed the project to TUBITAK, and upon securing a limited grant, a proof-of-concept study was initiated. The proposed design for resisting blast forces presents several advantages, including a lightweight structure relative to existing alternatives and a high strength-to-weight ratio. The prefabricated composite panel is sufficiently light for transport by military cargo helicopters and light ground vehicles, making it a viable option for protection at borders and critical military installations. Additionally, the ability to manufacture these panels at remote locations enhances their practicality. Consequently, all parties involved had strong incentives to support this study.

However, this broad spectrum of engagements was accompanied by a set of rules, regulations, limits, and deadlines that varied significantly between the government, academia, private sector, and military. The available testing time and explosive content were constrained to half a day, with 4 kg of C4 allocated for only four blast load tests. Requests from the author for additional time and tests were declined. The military grounds could solely be utilised for testing, not for sample investigations. Consequently, the only available photographs were taken before and after the explosion tests. The samples were retained on military grounds and later transferred to private sector premises for further investigation. Unfortunately, some photographs of the second composite plate obtained during this investigation were unavailable.

This was a proof-of-concept study involving panels at various stages. The design of the panels required three months, followed by an additional three months for initial factory tests to evaluate production and factory mobility. Static load tests and proof-of-concept evaluations for the mechanical design necessitated another two months. The external steel plates, mechanically connected to the concrete core through shear studs, performed as intended, providing external reinforcement akin to that of the concrete core. The bearing interaction between the concrete and steel studs was evident, with localised compressive failure observed on the concrete in contact with the steel studs. Static failure of the plates occurred due to the fracture of the concrete core, which remained attached to the steel plates.

The final stage of the proof-of-concept involved conducting the actual blast-load tests, which required an additional two months for organisation. The testing facility was fully booked, and the availability of time and resources necessitated considerable effort. Two composite panels were bolted at each end of the frame, providing catenary support if required. The panels successfully withstood all tests, although the final test resulted in extensive, localised damage. As anticipated, the internal area surrounding the blast charge sustained severe damage, but this remained confined within the panels, which effectively contained the fracture zone between the plates. This study demonstrates that a composite panel design, with external steel plates serving as tensile support and confinement for the concrete core, is valid. The inclusion of steel fibres in the confined concrete enhances its energy-absorption capacity, while the steel plates contribute additional energy absorption due to their plasticity.

Had the author possessed sufficient budget, time, resources, and managerial experience, more tests with sophisticated instrumentation could have been conducted. The time or means to perform an in-depth analysis of the plastified steel plates were unavailable. Volumetric analyses and mechanical tests of the samples obtained from the penetrated steel plates would have indicated the energy absorbed during the blast. Some pulverised concrete was lost during transport; although a granulometric analysis was conducted on the remaining fractured concrete, a comprehensive analysis would have provided insights into the total volume destroyed by the explosion and, consequently, the energy absorbed during fracture and pulverisation. Such detailed correlations between the damaged material and the input energy could quantitatively characterise the relationship between explosion action and structural response. The implementation of high-frequency response strain gauges at the support points and along the panels could have captured the bending reactions and catenary action of the panels during the blast forces. During the material design phase, displacement-based stress-strain analyses of the designed concrete material at variable loading rates would have provided a better representation of the design material.

Despite these limitations, this study successfully achieved its goal within a 12-month period: proving the design principle underlying the prefabricated panels. The intrinsic mechanical qualities imparted by the design were validated during the blast tests. The proposed composite panel design offers a high strength-to-weight ratio and presents a viable solution for enhancing the security of military and civilian structures against explosive threats.

## REFERENCES

[1] Goel, D.M., Matsagar, V.A.: Blast-Resistant Design of Structures, Practice Periodical on Structural Design and Construction, 19 (2013) 2.

[2] Olmati, P., Trasborg, P., Naito, C.J., Bontempi, F.: Blast resistant design of precast reinforced concrete walls for strategic infrastructures under uncertainty, International Journal of Critical Infrastructures, Inderscience Enterprises Ltd, 11 (2015) 3, pp. 197-212.

[3] ACI PRC-370-14: Report for the Design of Concrete Structures for Blast Effects, 2014.

[4] Shi, Y., Xiong W., Li, Z.X., Xu, Q.: Experimental studies on the local damage and fragments of unreinforced masonry walls under close-in explosions, International Journal of Impact Engineering, 90 (2016), pp. 122-131.

[5] Shi, Y., Wang, J., Cui, J.: Experimental studies on fragments of reinforced concrete slabs under close-in explosions, International Journal of Impact Engineering, 144 (2020).

[6] Mahima, G.R., Shivamanjunathaswamy, H.G., Kiran, T.: Behavior of steel concrete composite wall panel under blast load, International Research Journal on Advanced Engineering Hub, 2 (2024) 6, pp. 1768-1775.

[7] Dusenberry, D.: Anticipating the Post Blast Conditions of Structures, Canadian Journal of Civil Engineering, 36 (2009), pp. 1340-1344.

[8] Bischoff, P.H., Perry, S.H.: Compressive behavior of concrete at high strain rates, Matériaux Et Constructions, 24 (1991) 6, pp. 425-450.

[9] Gebbeken, N., Greulich, S., Pietzsch, A.: Performance of Concrete Based Building Materials Against Blast and Impact, Proceedings of the fib-Symposium on Concrete and Environment, Berlin, 2001.

[10] Dusenberry, D.: Handbook for Blast Resistant Design of Buildings, John Wiley and Sons, 2010.

[11] Draganić, H., Varevac, D.: Numerical simulation of effect of explosive action on overpasses, GRAĐEVINAR, 69 (2017) 6, pp. 437-451, https://doi.org/10.14256/JCE.1943.2016

[12] Ning, J., Yang, S., Ma, T., Xu, X.: Fragment behavior of concrete slab subjected to blast loading, Engineering Failure Analysis, 138 (2022) 8.

[13] Gebbeken, N., Döge, T.: Explosion Protection-Architectural Design, Urban Planning and Landscape Planning, International Journal of Protective Structures, 1 (2010) 1.

[14] Yu, R., Spiesz, P., Brouwers, H.J.H.: Energy absorption capacity of a sustainable Ultra-High Performance Fibre Reinforced Concrete [UHPFRC] in quasi-static mode and under the high-velocity projectile impact, Cement and Concrete Composites, 68 (2016), pp. 109-122.

[15] Lai, J., Sun, W.: Dynamic behaviour and visco-elastic damage model of ultra-high performance cementitious composite, Cement and Concrete Research, 39 (2009) 11, pp. 1044-1051.

[16] Grote, D.L., Park, S.W., Zhou, M.: Dynamic behavior of concrete at high strain rates and pressures: I. experimental characterization, International Journal of Impact Engineering, 25 (2001) 9, pp. 869-886.

[17] Bounds, W.: Concrete and Blast Effects, ACI International, SP-175.

[18] Elmezaini, N., Ashour, M.: Nonlinear Analysis of Concrete Beams Strengthened with Steel Fiber-Reinforced Concrete Layer, Journal of Engineering Research and Technology, 2 (2015) 3.

[19] Erdem, R.T., Berberoğlu, M., Gücüyen, E.: Investigation of concrete slabs made with cement based mortars under impact loads, GRAĐEVINAR, 75 (2023) 2, pp. 117-127, https://doi.org/10.14256/JCE.3159.2021

[20] Venkatesh, K.: Properties of Concrete at Elevated Temperatures, International Scholarly Research Notices, 2014, Article ID 468510, 15 pages.

[21] Guide to Thermal Properties of Concrete and Masonry Systems, ACI 122R-02, American Concrete Institute, 2002.

[22] Miller, D., Ho, N.M., Talebian, N., et al.: Real-time monitoring of early-age compressive strength of concrete using an IoT-enabled monitoring system: an investigative study, Innov. Infrastruct. Solut., 8 (2003) 75.

[23] FIB, N° 42.: Constitutive modelling for high strength / high performance concrete, State-of-art report, ISBN 978-2-88394-082-6, January 2008

[24] Nilson, A.: Design of Concrete Structures, WCB McGraw-Hill, (1997) 12. pp.77-79.